Polymer 51 (2010) 1593–1598

Contents lists available at ScienceDirect

Polymer

journal homepage: www.elsevier.com/locate/polymer

Controlling melt reactions during preparing long chain branched polypropylene using copper *N*,*N*-dimethyldithiocarbamate

Zhenjiang Zhang [a,b], Haiping Xing [a,b], Jian Qiu [a], Zhiwei Jiang [a,b], Haiou Yu [a,b], Xiaohua Du [a,b], Yanhui Wang [a], Li Ma [a], Tao Tang [a,*]

[a] *State Key Laboratory of Polymer Physics and Chemistry, Changchun Institute of Applied Chemistry, Chinese Academy of Sciences, Changchun 130022, PR China*
[b] *Graduate School of the Chinese Academy of Sciences, Beijing 100039, China*

ARTICLE INFO

Article history:
Received 4 October 2009
Received in revised form
24 December 2009
Accepted 29 January 2010
Available online 4 February 2010

Keywords:
Long chain branch
Melt reaction
Polypropylene

ABSTRACT

Effect of copper *N*,*N*-dimethyldithiocarbamate (CDD) on melt reactions during preparing long chain branched polypropylenes (LCB-PP) via free radical grafting was studied. The structure and rheological properties of the modified PPs were characterized. The results showed that CDD could efficiently control two side reactions, i.e. degradation of PP backbone and homopolymerization of multifunctional monomer (trimethylol propane triacrylate (TMPTA)) in the presence of peroxide. Meanwhile the addition of CDD also increased the efficiency of forming LCB structure. The reaction between CDD and active free radicals (carbon centered and alkoxy species) led to forming *in situ* dithiocarbamate radicals, which cannot attack PP backbone and are weaker initiator for TMPTA. The resultant dithiocarbamate radicals could react with the PP macroradicals and the acrylic radicals reversibly, which prolong the life time of PP macroradical and increase the reaction probability between macroradicals. The obtained LCB-PP showed high melt strength.

1. Introduction

Topological structure of macromolecules strongly influences properties of polymers, such as melt properties [1–3]. For example, linear polypropylene (PP), an important commercial polymer prepared by Ziegler–Natta catalysts, is often unsuitable for extensional flow processing due to its low "melt strength", but the situation can be improved significantly in the presence of even limited long chain branching (LCB) [4–7]. Importantly, long chain branched PP (LCB-PP) shows strain hardening in elongational flow due to its very long terminal relaxation time [4,8–11] which is required in the thermoforming processing. Thus varying the molecular architecture is one of the most effective methods of tailoring processing characteristics and end-product properties of polymers.

So far there are several approaches for preparing LCB-PP, such as *in situ* polymerization in a reactor [6,11,12], high-energy irradiation [5,13] and melt free radical grafting [14–20]. The third method is very convenient, in which three reactants, including PP, multifunctional monomer (as a graft monomer) and free radical initiator (usually using peroxide), are used to form LCB-PP via radical reaction. There are several reactions during the preparation of LCB-PP. The first step is the thermal decomposition of peroxide to form primary radicals (RO•). The following step is the abstraction of a hydrogen atom from PP backbone by a RO• leading to the formation of a macroradical. The macroradicals can further undergo β-scission or react with PP and multifunctional monomer. Generally, the LCB-PP is formed through recombining macroradicals whatever directly or indirectly via multifunctional monomer. Among the above reactions, β-scission of macroradicals and the homopolymerization of multifunctional monomers are undesirable side reactions [14]. The former will lead to chain cleavage and even severe degradation of PP at high temperature, which will result in the reduction of the melt strength of PP. The latter will result in uneven reactions between primary radicals/macroradicals and multifunctional monomers, and even the formation of highly branched structures or large gel aggregates. More importantly, polymer architectures with highly branched structures, such as hyperbranched polymers, make it difficult for these macromolecules to entangle [21], which also leads to the reduction of the melt strength. Therefore how to control the two side reactions is a key scientific issue in order to efficiently prepare LCB-PP. Prolonging the life time of macroradicals by forming reversible radicals using thiuram disulfides [14] or stabilizing macroradicals by changing radical intermediate states using styrene [22–24] and furan derivatives [25] are efficient routes to reduce the chain scission and

* Corresponding author. Tel.: +86 431 85262004; fax: +86 431 85262827.
E-mail address: ttang@ciac.jl.cn (T. Tang).

0032-3861/$ – see front matter © 2010 Elsevier Ltd. All rights reserved.
doi:10.1016/j.polymer.2010.01.063

improve grafting reaction. However, there is no report on inhibiting homopolymerization of multifunctional monomers during the preparation of LCB-PP via melt free radical grafting.

In this work, we report our effort to using a metal dithiocarbamate to control the two side reactions during preparing LCB-PP by melt grafting reaction. Here a triacrylate monomer is used as a multifunctional monomer in order to form branched structure. Copper *N*,*N*-dimethyldithiocarbamate (CDD) is used as a co-reactant not only to stabilize macroradicals but also to prohibit the homopolymerization of triacrylate monomer.

2. Experimental part

2.1. Materials

Polypropylene (PP, with a melt flow rate of 2.7 g/10 min) powder was supplied by Daqing Petrochemical Corporation, China. 2,5-Dimethyl-2,5(tert-butylperoxy) hexane (DHBP) peroxide was obtained from Aldrich. Trimethylol propane triacrylate (TMPTA) was obtained from Tianjin Tianjiao Chemical Co., China. Copper *N*,*N*-dimethyldithiocarbamate (CDD) was supplied by Puyang Weilin Chemical Co., China. Atactic polypropylene (a-PP, $M_w = 10{,}000$ g/mol, polydispersity = 2.0) was supplied by Scientific Polymer Products, Inc.

2.2. Preparation of samples

A co-rotating twin screw extruder (PRISM TSE 24 MC) with a 24 mm diameter and a 44:1 length-to-diameter ratio was used to prepare samples. The temperature in the first zone was set to 185 °C and in others was set to 220 °C with a temperature of 230 °C for the die (7 heating zones). The screw rotating speed was 100 rpm. In order to make the additives dispersed evenly in PP powder, the peroxide, TMPTA and Irganox B215 were dissolved in acetone, and then the solution was added to PP powder in a vessel, and a known amount of CDD was added at the same time. The vessel was stirred for 20 min. At last, the mixture was placed in ventilating cabinet at room temperature until the acetone volatilized completely.

The reaction between a-PP (4 g) and CDD (0.04 g) in the presence of DHBP (0.1 mL) was done at 160 °C for 15 min under N_2 atmosphere. The resultant product was dissolved in *n*-hexane. The residual CDD and other insoluble byproducts were eliminated by filtration. The solution was charged into ethanol, and the precipitate from ethanol was dried under vacuum for 24 h at 45 °C. The purified product was used as a model for the structural analysis.

2.3. Characterization

Molecular weight was measured by high-temperature size-exclusion chromatography (HTSEC) coupled with a two-angle laser light scattering (TALLS) detector and a refractive index detector (model: PL-GPC-220). By coupling HTSEC with TALLS, the absolute molar mass M_{LS} and the radius of gyration (R_g) of every fraction can be determined directly. The ratio of the mean-square radius of gyration of a branched polymer $< R_g^2 >_{br}$ to that of a linear polymer $< R_g^2 >_{lin}$ of the same molecular weight is the so-called Zimm–Stockmayer branching parameter g [26]:

$$g = \frac{< R_g^2 >_{br}}{< R_g^2 >_{lin}} \tag{1}$$

For the chemical modified polypropylene, a trifunctional randomly branched architecture can be assumed preferentially by statistic [16,17]. For such a trifunctional randomly branched polymer, g can be related to branching by

$$g = \left[\left(1 + \frac{m}{7}\right)^{0.5} + \frac{4m}{9\pi}\right]^{-0.5} \tag{2}$$

with m as the number of branching sites along the molecule [26]. From that the number of long-chain branches per 1000 monomer units (λ) is determined as

$$\lambda = \frac{m}{M} \times 1000 \times M_M \tag{3}$$

where M_M is the molar mass of the monomer unit and M is molar mass of branched polymer.

^{1}H NMR spectra were recorded on a Varian Unity 400 MHz instrument in chloroform-D. The grafting degree of TMPTA in modified PP was measured using FTIR (Bio-Rad FTS135 spectrophotometer). Before measurements, the modified samples were extracted in boiling xylene for 8 h. The extracted solution was charged into acetone at room temperature and the precipitates were filtrated. The precipitates were pressed into films for FTIR measurements after dried at 70 °C for 20 h under vacuum.

Thermal analysis-Fourier transform infrared spectroscopy (TGA-FTIR) on a AST-2 instrument (Perkin–Elmer) connected to the FTIR of Thermo Nicolet 6700 was used to monitor the decomposition products at different temperature. The measurement procedure was as follows: the samples were quickly heated from 30 °C to 150 °C at the rate of 20 °C/min, then heated to 200 °C at the rate of 5 °C/min to avoid temperature overshoot, at last kept at 200 °C for 10 min. The total testing time was 26 min. Dry nitrogen gas with a flow of 50 mL/min carried the decomposition products through steel tubing into the gas cell for IR detection. Both the transfer line and the gas cell were kept at 220 °C to prevent gas condensation.

Thermogravimetric analyses (TGA) were done by Thermal Analysis Instrument (SDTQ600, TA Instruments, America) from 30 to 500 °C under air with a heating rate of 10 °C/min. Melting points (T_m) and crystallization temperature (T_c) of the samples were determined by differential scanning calorimetry (DSC) performed on a Perkin–Elmer DSC-7 instrument, using a heating rate of 10 °C/min in the temperature range 40–200 °C under nitrogen.

A rotation rheometer (Physica MCR-300 rheometer with a 25 mm parallel plate arrangement) was used for rheological measurements at 180 °C. The rheometer oven was purged with dry nitrogen to avoid degradation of samples during measurement. A frequency range of 0.01–100 rad/s and a strain of 1% which was in the linear viscoelastic regime for all samples were applied.

3. Results and discussion

The molecular weights of plain PP and the modified PP samples were measured by HTSEC with light scattering detector. Compared to plain PP, the number-average molecular weight (M_n) of PP12 decreased obviously due to the degradation of PP backbone initiated by the added peroxide (DHBP). In contrary, the M_n of CPP12 was higher than that of plain PP (Table 1), indicating that the β-scission of PP backbone was controlled by the addition of CDD. The molecular weight distribution curves are shown in Fig. 1. There was a small peak at higher molecular weight region when CDD was used for modification.

The dependence of the radius of gyration (R_g) on the molecular weight for plain PP and the modified PP samples is shown in Fig. 2a. The slope of the curve for plain PP was 0.6, which is in accordance with the result of Auhl [5]. The R_gs of both PP12 and CPP12 were lower than that of plain PP in high molecular weight region, meaning that the LCB was introduced onto PP backbone. The branching parameter (g) of PP12 was higher at low molecular weight but lower at high molecular weight than that of CPP12. This

Table 1
Structural parameters and melt properties of PP and modified PPs.

Sample	M_n (Kg/mol)	M_w/M_n	GD[a] (wt%)	η_0[b] (Pa·s)	MS[c] (cN)	Gel[d] (wt%)
PP	152	2.93	0	19680	2	0
PP12[e]	115	3.43	1.03	2360	1	0
CPP12[f]	207	2.72	0.86	77120	22	0
CPP[g]	136	2.71	0	10500	1.5	0

[a] Grafting degree of TMPTA.
[b] The zero shear viscosity was determined by extrapolating to 0.001 rad/s in the plots of complex viscosity vs angular frequency.
[c] Melt strength measured by a Gottfert Rheotens device in combination with a high pressure capillary rheometer.
[d] The content of gel.
[e] [DHBP] = 3.4 mmol/kg; [TMPTA] = 40.5 mmol/kg; [B215] = 2 g/kg.
[f] [DHBP] = 3.4 mmol/kg; [TMPTA] = 40.5 mmol/kg; [CDD] = 1.6 mmol/kg; [B215] = 2 g/kg.
[g] [DHBP] = 3.4 mmol/kg; [CDD] = 1.6 mmol/kg; [B215] = 2 g/kg.

shows that the distribution of branched chains is more non-uniform within PP12 chains with different molecular weight comparing with that of CPP12. The long chain branch frequency (λ, i.e. the number of LCB per 1000 monomers) was calculated. Fig. 2b shows the λ as a function of molecular weight for both PP12 and CPP12. The value of λ increased with increasing molecular weight of the modified PP samples. This result is similar to that of Parent [27], who thought that multifunctional monomer was preferentially grafted to the chains with high molecular weight in a coagent-mediated system. As a result, more LCB will be formed in PP chains with high molecular weight. In high molecular weight region, the λ of PP12 was higher than that of CPP12. These might result from the homopolymerization of TMPTA in the absence of CDD. Because there are three carbon–carbon double bonds (C=C) in the TMPTA molecule, the grafted TMPTA on the PP backbone has two more C=C that can react with active free radicals. As a result, polymer architectures of highly branched structures will be easily formed during melt processing if the homopolymerization of TMPTA occurs in the systems. In contrary, the homopolymerization of TMPTA was probably controlled by CDD in the case of CPP12, leading to the lower amount of TMPTA grafted to PP backbone.

Model experiments were done to investigate the influence of CDD on the homopolymerization of TMPTA. In the case without DHBP, TMPTA did not polymerize at 180 °C for 7 min in the presence of a small amount of CDD; however, TMPTA alone polymerized to form a piece of solid crosslinked polymer under the same conditions. In the cases with DHBP, although TMPTA could polymerize in the presence of CDD, the addition of CDD obviously

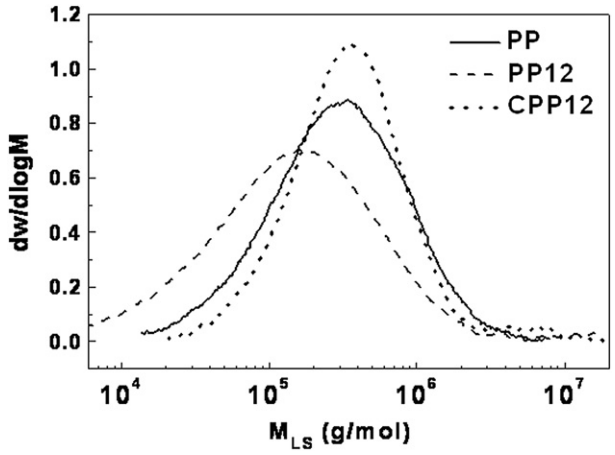

Fig. 1. Molecular weight distribution curves of PP and the modified PP samples.

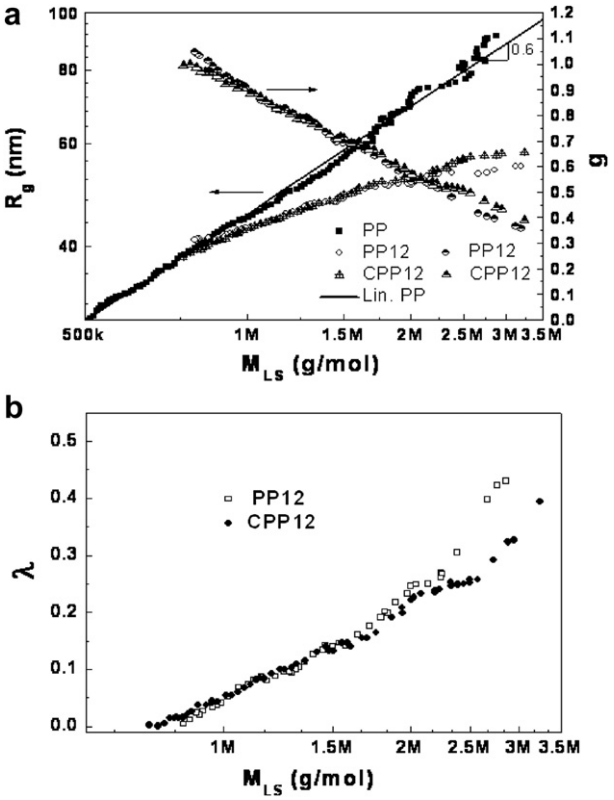

Fig. 2. (a) The radius of gyration (R_g) and branching parameter (g) vs. the molecular weight (M_{LS}); (b) The number of long chain branches per 1000 monomers (λ) vs. M_{LS} for the modified PP samples measured by SEC-TALLS.

delayed the homopolymerization of TMPTA. This indicates that the homopolymerization of TMPTA can be controlled by CDD.

FTIR spectra of the purified samples are shown in Fig. 3. For the samples modified with TMPTA, there was a band at about 1740 cm^{-1} due to the stretching vibration of carbonyl group of the ester in the grafted TMPTA molecule, indicating that TMPTA was grafted onto PP backbone. In order to quantify the reacted TMPTA, the carbonyl index (CI) was calculated as follows:

$$CI = \frac{A_{1740}}{A_{1167}} \quad (4)$$

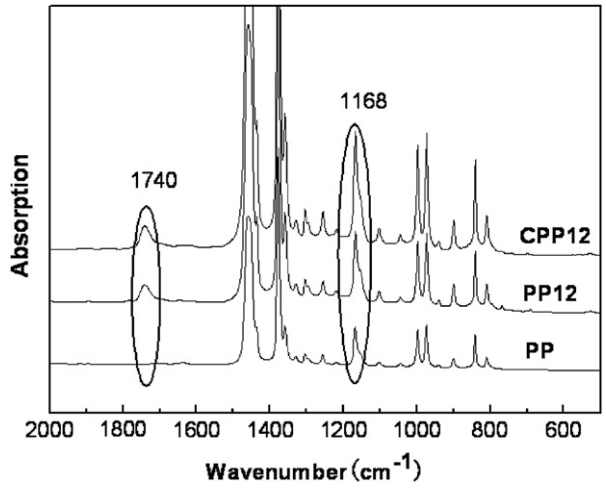

Fig. 3. FTIR spectra (500–2000 cm^{-1}) of plain PP and the modified PP samples after purification.

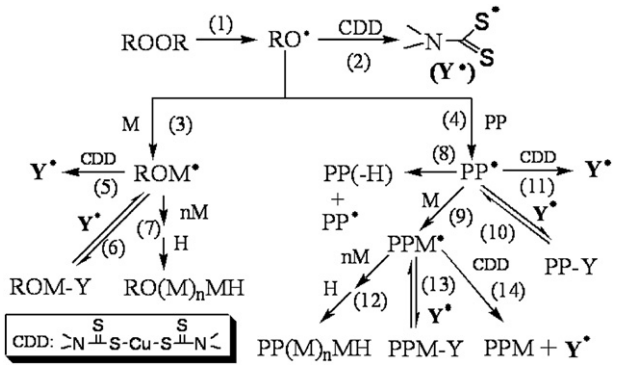

Fig. 4. Schematic drawing of possible important chemical reactions in the presence of CDD (M: TMPTA).

where A_{1740} is the absorbance at 1740 cm^{-1}, characteristic of carbonyl group of the ester in the TMPTA molecules; and A_{1167} is the absorbance at 1167 cm^{-1}, characteristic of the CH_3 groups (stretching of C–CH_3 groups on PP chains) [25], which is proportional to the amount of PP. The CI can be considered as a measure of the content of grafted TMPTA (either in a single unit or poly chains) on the PP backbone. Because this method is the relative measurement, in order to achieve the grafting degree (GD), a calibration curve was constructed. The mixtures with known amounts of TMPTA and PP were prepared by melt mixing to establish the calibration curve. According to the results of FTIR and the calibration curve, the grafting degree of TMPTA in the PP12 was 1.03 wt% (Table 1), which is higher than that of CPP12 (0.86 wt%). This conforms to the analysis mentioned-above.

Fig. 4 shows a possible reaction mechanism for controlling the degradation of PP and homopolymerization of TMPTA by CDD. Holdsworth et al. reported that the reaction between metal dithiocarbamates and hydroperoxide maybe release dithiocarbamate radicals [28]. Here we consider that the CDD could also release dithiocarbamate radical by reacting with active free radicals whether they are carbon centered radical or alkoxy species. The results of TGA showed that the temperatures of both DHBP and CDD at the maximum loss mass deceased obviously, especially that of CDD (Fig. 5). In order to clarify the reaction between DHBP and CDD, TGA-FTIR analysis was performed to investigate the gaseous products of CDD, DHBP, and CDD/DHBP under a nitrogen atmosphere. There was almost no weight loss for CDD from 30 °C to 200 °C. Thus there were no signals detected by FTIR. Fig. 6 shows the FTIR spectra of gaseous products of DHBP and DHBP/CDD at 14.3 min (~191.5 °C). Compared to DHBP, there were two new peaks at 987 cm^{-1} and 1145 cm^{-1} for DHBP/CDD. According to the previous results [29], the band at 1145 cm^{-1} can be assigned to the

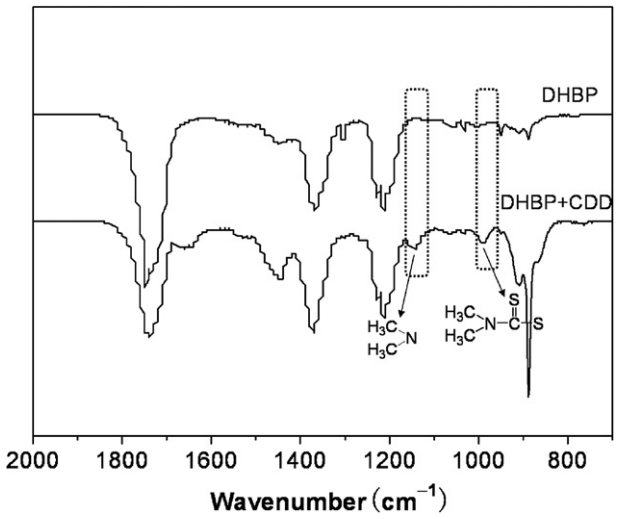

Fig. 6. FTIR spectra of gaseous products of DHBP and DHBP/CDD mixture at 14.3 min.

group of CH_3–N, and the band at 987 cm^{-1} can be assigned to the group of $(CH_3)_2$N–CSS. Fig. 7 shows the FTIR spectra of gaseous products of DHBP/CDD at different time. The intensities of characteristic peaks at 987 cm^{-1} and 1145 cm^{-1} increased at first and then decreased. This tendency was consistent with the change trend of the concentration of the primary radicals produced by peroxide (DHBP). In addition, from DTG curves (Fig. 5b), the temperature with the maximum mass loss rate for CDD in the DHBP/CDD mixture was 206 °C (332 °C for pure CDD), in which most of the DHBP was decomposed. This means that the decomposition of CDD at 206 °C is not related to the presence of DHBP. Therefore, the decomposition of CDD should result from the reaction between CDD and the residual primary radicals in the gas phase. According to the above results, the dithiocarbamate radical should be formed by the reaction between CDD and the primary radicals produced by peroxide, as shown in Fig. 4.

Similarly the reactions between CDD and active free radicals (such as the reactions of (2), (5), (11) and (14) in Fig. 4), which are the key factors to hinder the above side reactions, should take place. By reacting with CDD, a part of active free radicals will become dithiocarbamate radicals *in situ*. However, the dithiocarbamate radical is a weak initiator of acrylate monomer [30]. In a comparative experiment, the addition of thiuram disulfide alone (such as TMTD, which releases two dithiocarbamate radicals at high temperature) did not result in the decrease of molecular weight of PP after extrusion at 220 °C comparing plain PP. Consequently, the PP skeleton should be not attacked by the dithiocarbamate radicals. Therefore the instantaneous concentration of active free radicals

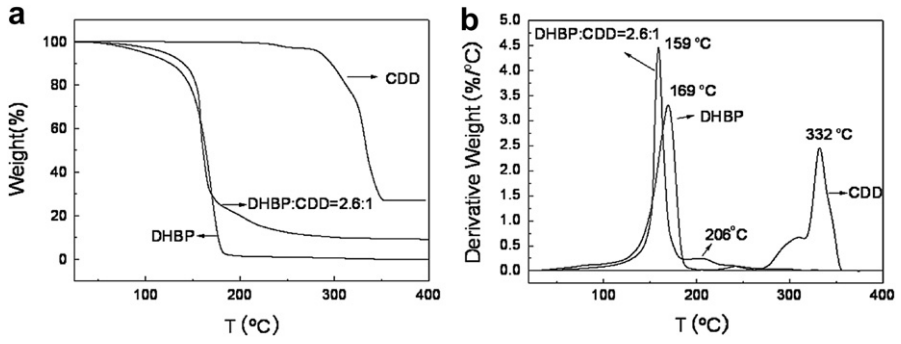

Fig. 5. TGA (a) and DTG (b) curves for DHBP, CDD and DHBP/CDD = 2.6/1 (molar ratio) mixture.

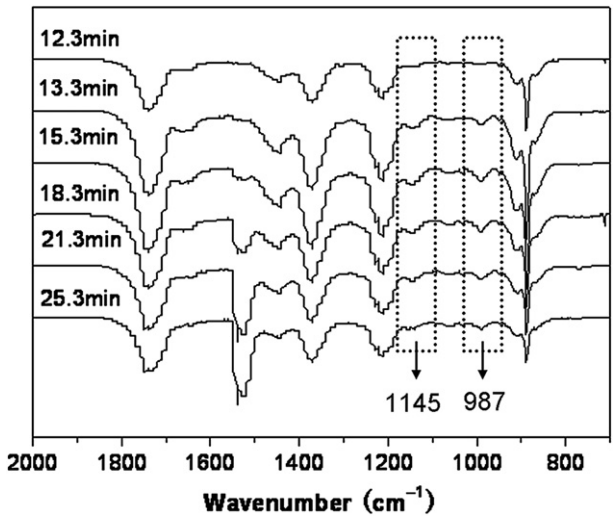

Fig. 7. FTIR spectra of gaseous products of DHBP/CDD mixture at different time.

attacking PP backbone and TMPTA is decreased in the presence of CDD, and the degradation of PP backbone and the homopolymerization of the TMPTA can be controlled. However, the dithiocarbamate radicals could react with PP macroradicals and acrylic radicals, such as the reactions of (6), (10) and (13) in Fig. 4. The reaction between PP radical and dithiocarbamate radical (the reaction (10) in Fig. 4) was confirmed by the data of ^{1}H NMR using a model experiment. After a-PP reacted with the mixture of DHBP and CDD at 160 °C for 15 min, there was a minor chemical shift at 3.72 ppm for the modified a-PP after purification (Fig. 8), which corresponds to the CH_3 in the group of $(CH_3)_2$N–CSS. Furthermore, these reactions are reversible, which can prolong the life time of macroradicals. Thus the presence of dithiocarbamate radicals can also increase the reaction probability between macroradicals and macroradicals (or the grafted TMPTA). Another comparative experiment further confirmed the inhibition of CDD on the degradation of PP via the reactions of (10) and (11) in Fig. 4. After adding CDD in the PP containing DHBP, the M_n of the sample (CPP in Table 1) was between those of plain PP and PP12. From Fig. 4, owing to the reactions between CDD and active free radicals, the addition of CDD is more efficient to control the side reactions during preparing LCB-PP by melt grafting, compared with the addition of thiuram disulfides [14].

Rheological measurements also confirmed the above analysis about the reactions in the systems. Fig. 9a shows the plots of complex viscosity (η^*) as a function of angular frequency (ω). Compared to plain PP, adding both DHBP and TMPTA (in the case of PP12) led to an obvious reduction of η^* in all the frequency region due to dramatic degradation of PP chains, but adding both DHBP and CDD (in the case of CPP) resulted in a slight decrease of η^* in the low frequency region. This shows the controlling effect of CDD on the degradation of PP chains due to the strong capacity of CDD and its derivatives (dithiocarbamate radicals) for trapping active free radicals. In contrast, compared to other samples, the η^* in the low frequency region increased obviously in the case of CPP12 (containing DHBP, TMPTA and CDD simultaneously). Tsenoglou used zero shear viscosity (η_0) to estimate the branching degree of modified samples [17]. The presence of LCB in a sample will result

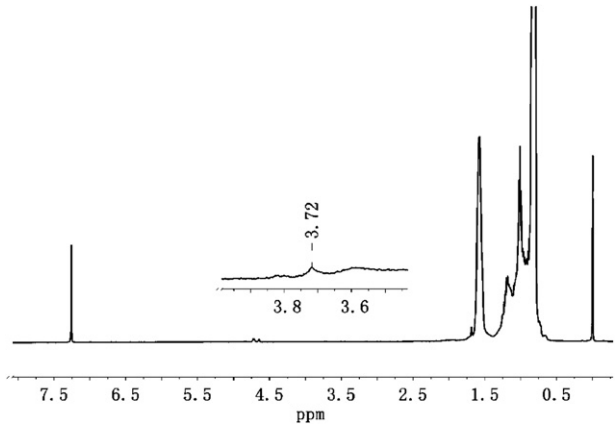

Fig. 8. ^{1}H NMR spectra of purified a-PP in chloroform-D after reaction with DHBP and CDD at 160 °C for 15 min.

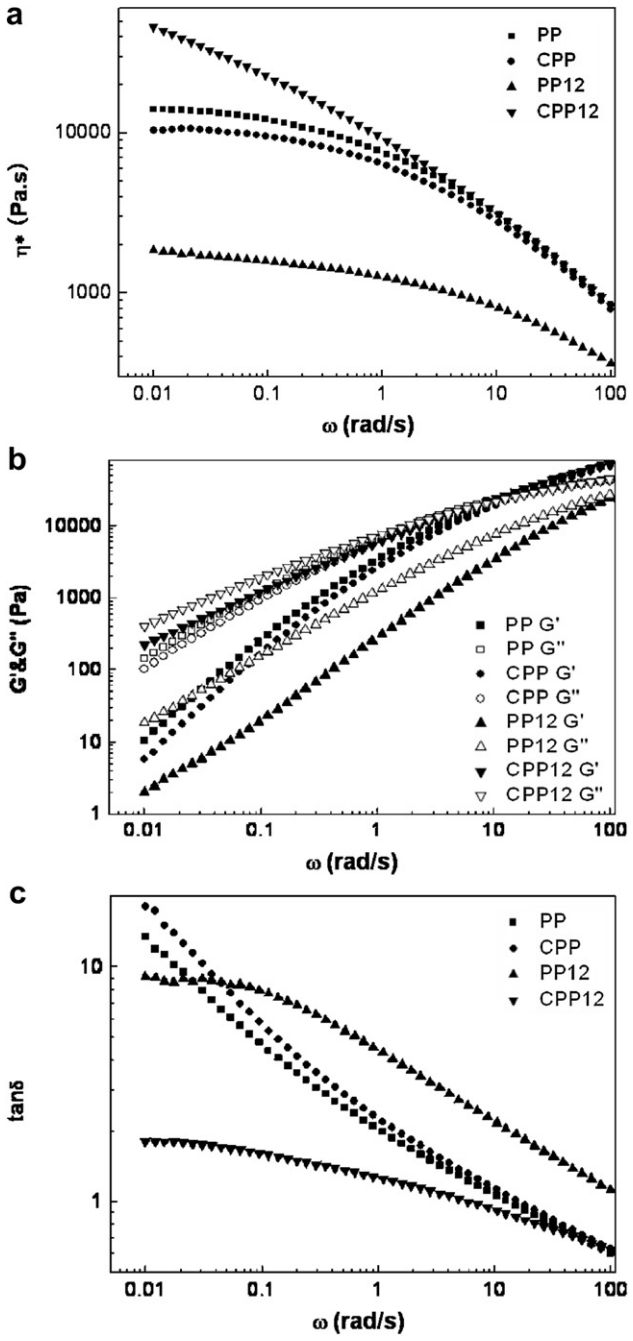

Fig. 9. Rheological data of plain PP and modified PP at 180 °C: (a) Complex viscosity vs. angular frequency, (b) Storage modulus G' and loss modulus G'' vs. angular frequency, (c) tan δ vs. angular frequency.

Table 2
Crystalline properties and thermal stabilities of PP and the modified PPs[a].

Sample	T_m (°C)	T_c (°C)	$T_{5\%}$ (°C)	T_{max} (°C)
PP	165.2	116.4	259.6	334.1
CPP	164.7	116.4	263.7	373.4
PP12	164.1	118.2	267.2	346.9
CPP12	165.2	121.4	268.0	380.6

[a] Crystalline properties were measured by DSC under nitrogen; thermal stabilities were measured by TGA under air.

in an obvious increase of η_0. Table 1 shows that the η_0 of CPP12 is much higher than those of other samples. This means that the LCB structure has been formed in the CPP12. Comparatively, although the η_0 of CPP was lower than that of plain PP, it was still higher than that of PP12. In the case of PP12, severe degradation of PP backbone and the formation of high branched structures resulting from the homopolymerization of TMPTA led to the dramatic reduction of melt viscosity.

Fig. 9b shows the storage modulus (G') and loss modulus (G'') vs. angular frequency (ω) of plain PP and the modified PP samples at 180 °C. The G' at the low frequency, reflecting the longest relaxation time, is very sensitive to the topological structure of macromolecules. The value of G' for CPP12 is the highest among all the samples at low frequency (Fig. 9b). The plain PP exhibited the typical terminal behavior with the terminal slope of 1.71. The CPP12 showed the smallest terminal slope of G' (0.74), suggesting that CPP12 has the longest relaxation time among all the samples. This is ascribed to the LCB or even crosslinking structures formed via radical reactions. The extraction experiments showed that there was no gel in all the samples (Table 1), implying that severe crosslinking did not occur in the samples. Thus the change of rheological behavior in the CPP12 should result from the formation of the LCB structures. Compared to the G', the G'' is less affected by the formation of branches. Because of the dramatic degradation of PP chains, there is no crossover between G' and G'' curves of PP12 in examined frequency region. For CPP, the crossover between G' and G'' curves horizontally shifted to a little higher frequency, indicating a mild degradation. For CPP12, the crossover showed a horizontal shift to lower frequency and a vertical shift to low value of G' (or G''). Yamaguchi et al. attributed this phenomenon to the existence of LCBs [31].

The tan δ as a function of angular frequency (ω) is shown in Fig. 9c. For linear polymers, plain PP and CPP, the tan δ ascended quickly with the reduction of angular frequency. With the addition of peroxide and TMPTA (in the case of PP12), tan δ was higher at high frequency and lower at low frequency compared with plain PP. With the addition of peroxide, TMPTA and CDD (in the case of CPP12), the value of tan δ decreased obviously at low frequency, which was much lower than those of linear samples. This observation was in accordance with the results of Graebling [14] and Tian [16], who attributed the phenomenon to the grafting of LCB onto PP backbone. As expected, LCB-PP with high melt strength was successfully prepared through melt grafting in the presence of CDD (Table 1).

Crystalline properties and thermal stabilities of PP and the modified PPs were compared by means of DSC and TGA (Table 2). Although the melting point (T_m) of all the samples almost did not change, the presence of LCB structure in the modified PPs (CPP12 and PP12) increased the crystallization temperature (T_c) of PP. This might result from the nucleation effect of branch sites on the crystallization of PP chains. Compared to plain PP, thermal stabilities of the modified PPs did not change under nitrogen atmosphere; however, their thermal stabilities were dramatically improved under air atmosphere, especially the temperature at the maximum mass loss rate (T_{max}). The T_{max} of CPP12 was 46 °C higher than that of plain PP.

4. Conclusion

The addition of CDD could obviously promote the efficiency of forming long chain branches on PP backbone and prohibit the degradation of PP during melt grafting. Meanwhile the homopolymerization of TMPTA could be also controlled. The reaction between CDD and active free radicals (carbon centered and alkoxy species) are the key factors to hinder the side reactions, i.e. the degradation of PP and the homopolymerization of TMPTA. On one hand, a part of active free radicals will *in situ* become dithiocarbamate radicals, which cannot attack PP backbone and is weaker initiator for TMPTA. So the instantaneous concentration of active free radicals is decreased, and the degradation of PP backbone and the homopolymerization of the TMPTA can be controlled. On the other hand, the dithiocarbamate radicals could react with the PP macroradicals and the acrylic radicals, and these reactions were reversible. Thus the presence of the dithiocarbamate radicals could prolong the life time of PP macroradical, which increase the reaction probability between macroradical and macroradical (or the grafted TMPTA). As expected, LCB-PP with high melt strength was successfully prepared through melt grafting in the presence of CDD. In addition, the thermal stabilities of LCB-PP were dramatically improved under air atmosphere comparing with that of plain PP.

Acknowledgements

We thank the financial supports from the National Natural Science Foundation of China for the projects (20734006, 50873099, 20804045 and 50921062) and the Ministry of Science and Technology of China (Project No. 2008AA03Z508).

References

[1] Yan D, Wang WJ, Zhu SP. Polymer 1999;40:1737–44.
[2] Wang WJ, Ye ZB, Fan H, Li BG, Zhu SP. Polymer 2004;45:5497–504.
[3] Liao RG, Yu W, Zhou CX. Polymer 2010;51:568–80.
[4] Lagendijk RP, Hogt AH, Buijtenhuijs A, Gotsis AD. Polymer 2001;42:10035–43.
[5] Auhl D, Stange J, Münstedt H, Krause B, Voigt D, Lederer A, et al. Macromolecules 2004;37:9465–72.
[6] Weng W, Hu W, Dekmezian AH, Ruff CJ. Macromolecules 2002;35:3838–43.
[7] Ratzsch M, Arnold M, Bosig E, Bucka H, Reichelt N. Prog Polym Sci 2002;27:1195–282.
[8] Weng W, Markel EJ, Dekmezian AH. Macromol Rapid Commun 2001;22:1488–92.
[9] Langston JA, Colby RH, Shimizu F, Suzuki T, Aoki M, Chung TCM. Macromol Symp 2007;260:34–41.
[10] Sugimoto M, Suzuki Y, Hyun K, Ahn KH, Ushioda T, Nishioka A, et al. Rheol Acta 2006;46:33–44.
[11] Langston JA, Colby RH, Chung TCM, Shimizu F, Suzuki T, Aoki M. Macromolecules 2007;40:2712–20.
[12] Paavola S, Saarinen T, Lofgren B, Pitkanen P. Polymer 2004;45:2099–110.
[13] Lugao AB, Otaguro H, Parra DF, Yoshiga A, Lima LFCP, Artel BWH, et al. Radiat Phys Chem 2007;76:1688–90.
[14] Graebling D. Macromolecules 2002;35:4602–10.
[15] Romani F, Corrieri R, Braga V, Ciardelli F. Polymer 2002;43:1115–31.
[16] Tian J, Yu W, Zhou CX. Polymer 2006;47:7962–9.
[17] Tsenoglou CJ, Gotsis AD. Macromolecules 2001;34:4685–7.
[18] Li SZ, Xiao MM, Wei DF, Xiao HN, Hu FZ, Zheng AN. Polymer 2009;50:6121–8.
[19] Parent JS, Bodsworth A, Sengupta SS, Kontopoulou M, Chaudhary BI, Poche D, et al. Polymer 2009;50:85–94.
[20] Mabrouk KE, Parent JS, Chaudhary BI, Cong RJ. Polymer 2009;50:5390–7.
[21] Sendijarevic I, McHugh AJ. Macromolecules 2000;33:590–9.
[22] Cartier H, Hu GH. J Polym Sci Part A Polym Chem 1998;36:2763–74.
[23] Cartier H, Hu GH. J Polym Sci Part A Polym Chem 1998;36:1053–63.
[24] Xie XM, Chen NH, Guo BH, Li S. Polym Int 2000;49:1677–83.
[25] Coiai S, Passaglia E, Aglietto M, Ciardelli F. Macromolecules 2004;37:8414–23.
[26] Zimm BH, Stockmayer WHJ. Chem Phys 1949;17:1301–14.
[27] Parent JS, Sengupta SS, Caufman M, Chaudhary BI. Polymer 2008;49:3884–91.
[28] Holdsworth JD, Scott G, Williams D. J Chem Soc 1964:4692–9.
[29] Anthoni U, Borch G, Klaeboe P, Nielsen PH. Acta Chem Scand 1978;32:705–14.
[30] Lambrinos P, Tardi M, Polton A, Sigwalt P. Eur Polym J 1990;26:1125–35.
[31] Yamaguchi M, Wagner MH. Polymer 2006;47:3629–35.